


LncRNA GAS5 Suppresses the Proliferation and Invasion of Osteosarcoma Cells via the miR-23a-3p/PTEN/PI3K/AKT Pathway

Cell Transplantation
Volume 29: 1–14
© The Author(s) 2020
Article reuse guidelines:
sagepub.com/journals-permissions
DOI: 10.1177/0963689720953093
journals.sagepub.com/home/ctj


Jianmin Liu¹, Ming Chen² , Longyang Ma¹, Xingbo Dang¹, and Gongliang Du¹

Abstract

Accumulating evidence has shown that long noncoding RNA GAS5 is a well-known tumor suppressor in the pathogenesis of a variety of human cancers. However, the detailed role of GAS5 in osteosarcoma is still largely unclear. In this study, we found that GAS5 was downregulated in human osteosarcoma tissues and cell lines compared with matched adjacent tissues and normal osteoblast cells. Overexpression of GAS5 could significantly suppress the growth and invasion of osteosarcoma cells, while downregulation of GAS5 promoted cell proliferation and invasion. We confirmed that GAS5 could directly bind with miR-23a-3p by using luciferase reporter gene and RNA immunoprecipitation and pull-down assay. Downregulation of miR-23a-3p repressed cell proliferation and invasion. Overexpression of miR-23a-3p counterbalanced the inhibition effect of GAS5 on cell proliferation and invasion. Further studies indicated that overexpression of GAS5 inhibited cell proliferation and metastasis by regulating phosphatase and tensin homolog (PTEN). PTEN was authenticated as a target of miR-23a-3p. Upregulation of GAS5 or silence of miR-23a-3p increased the level of PTEN, while downregulation of GAS5 or overexpression of miR-23a-3p suppressed the expression of PTEN. In addition, overexpression of GAS5 could neutralize the effect of downregulating PTEN on osteosarcoma cell functions. We proved that GAS5 regulated the viability and invasion of osteosarcoma cells through the PI3K/AKT pathway. Moreover, overexpression of GAS5 could inhibit tumor growth in a xenograft nude mouse model *in vivo*. In summary, GAS5 functions as a competing endogenous RNA, sponging miR-23a-3p, to promote PTEN expression and suppress cell growth and invasion in osteosarcoma by regulating the PI3K/AKT pathway.

Keywords

long noncoding RNA, growth arrest special 5, osteosarcoma, miR-23a-3p, phosphatase and tensin homolog

Introduction

Osteosarcoma is the most common malignant bone tumor which most frequently occurs in young adults and children and has a high rate of metastasis and recurrence^{1–3}. With the application of surgery combined with chemotherapy, the 5-year survival rate of patients with nonmetastatic osteosarcoma is between 60% and 70%, but the survival rate of patients with metastatic osteosarcoma is only 11%–13%^{4–6}. Therefore, it is urgent to elucidate the pathogenesis and molecular mechanisms of osteosarcoma, which will be helpful for the development of effective treatments of osteosarcoma.

Long noncoding RNAs (lncRNAs) are a class of protein-noncoding transcripts with a length greater than 200 nucleotides^{7,8}. Increasing evidence has revealed the important regulatory effects of lncRNAs on a variety of physiological and pathological processes, especially cancer^{8,9}. LncRNAs could serve as competing endogenous RNAs (ceRNAs) by

interfering with the expression of miRNAs involved in the occurrence and development of cancers. LncRNA growth arrest-specific transcript 5 (GAS5) has been demonstrated to be involved in several human cancers, and acts as a tumor suppressor¹⁰. An *in vitro* investigation revealed that GAS5 could suppress pancreatic cancer metastasis¹¹. In gastric

¹ Department of Emergency Surgery, Shaanxi Provincial People's Hospital (Affiliated Hospital of Xi'an Medical University), Xi'an, China

² Department of Orthopedics, Shaanxi Provincial People's Hospital (Affiliated Hospital of Xi'an Medical University), Xi'an, China

Submitted: May 4, 2020. Revised: July 27, 2020. Accepted: August 6, 2020.

Corresponding Author:

Ming Chen, Department of Orthopedics, Shaanxi Provincial People's Hospital (Affiliated Hospital of Xi'an Medical University), 256 Youyi West Road, Xi'an 710068, China.
Email: chenwn1911@163.com



cancer, overexpression of GAS5 suppresses tumorigenesis and development¹². However, the potential role of GAS5 in osteosarcoma is largely unknown.

It has been reported that lncRNAs could serve as ceRNAs by interfering with the expression of miRNAs to be involved in the occurrence and development of cancers^{2,5}. As is well known, miRNAs also could bind to different mRNAs to regulate the development of multiple tumors^{13,14}, including bladder cancer, pancreatic cancer, osteosarcoma, and so on^{15–17}. But the relationship between lncRNA and miRNA is not entirely clear yet¹⁸. Some research suggested that lncRNAs might sponge miRNAs to sequester miRNAs away from their target mRNAs^{2,19,20}. Hence, exploring the function of lncRNA–miRNA–mRNA crosstalk could be expected to become a key development in the mechanism and pathogenesis of cancers. MiR-23a-3p level was upregulated in a variety of tumors, indicating that miR-23a-3p could be involved in the occurrence and development of tumors²¹. Moreover, miR-23a-3p might promote tumor development by inhibiting the expression of phosphatase and tensin homolog (PTEN)²². In the view of these findings, we were interested in whether miR-23a-3p regulated the level of PTEN to be involved in the development of osteosarcoma.

In this study, we found the level of GAS5 in osteosarcoma was lower than that in adjacent tissues as in other tumors. Then, we explored the role and underlying mechanisms of GAS5 in osteosarcoma cells. Bioinformatics analysis, luciferase reporter gene RNA immunoprecipitation, and pull-down assay were used to determine the targeted interaction between GAS5 and miR-23a-3p. And the effect of GAS5 on miR-23a-3p/PTEN and PI3K/AKT signaling pathway was also investigated in osteosarcoma. Furthermore, *in vivo* xenograft experiment was used to explore the effect of GAS5 on osteosarcoma growth. This investigation may be an effective strategy for the treatment of osteosarcoma.

Materials and Methods

Clinical Specimens

Twenty osteosarcoma tissues and their matched adjacent tissues were collected from patients (15 males and 5 females; average age 19 years old) who received surgical treatment at the Shaanxi Provincial People's Hospital from February 2017 to November 2018. All the patients did not receive radiotherapy and/or chemotherapy before operation and gave informed consent before surgery. The histological diagnosis of osteosarcoma conformed to the World Health Organization's histological criteria for osteosarcoma and the protocols were approved by the Ethics Committee of Shaanxi Provincial People's Hospital. Tissues were frozen in liquid nitrogen immediately and stored at -80°C .

Cell Lines and Culture

Human normal osteoblast cells (hFOB1.19) and human osteosarcoma cell lines (Saos2, 143B, MG-63, U2OS, and

HOS) were purchased from American Type Culture Collection (ATCC, Manassas, VA, USA). All cells were incubated in Dulbecco's modified Eagle's medium (DMEM; Gibco, Rockville, MD, USA) containing 10% fetal bovine serum (Gibco) and 100 U/ml penicillin and 100 $\mu\text{g}/\text{ml}$ streptomycin (Sigma, St. Louis, MO, USA) at 37°C in a humidified atmosphere with 5% CO_2 .

Reverse Transcription-Quantitative Polymerase Chain Reaction

Total RNA was separated from tissues and cells using TRIzol reagent (Invitrogen, Carlsbad, CA, USA) according to the manufacturer's instructions. Briefly, tissues or cells were lysed with 600 μl of TRIzol, then the supernatant was precipitated with 600 μl of chloroform and isopropanol and washed with 75% ethanol. Finally, RNA precipitation was dissolved with RNase-free H_2O . RNA purity and integrity were analyzed by a spectrophotometer and Bio-Rad Experion automatic electrophoresis system (Bio-Rad, Hercules, CA, USA). RNA was reversely transcribed into cDNA using a PrimeScript RT reagent Kit (Takara Biotechnology, Dalian, China) and cDNA amplification was carried out using TaqManTM MicroRNA Reverse Transcription Kit (Applied Biosystems, Waltham, MA, USA) and PrimeScript RT Master Mix (Takara Biotechnology). Then 25- μl reaction system was built, containing 12.5 μl SYBR Premix Ex Taq II, 1.0 μl primers (10 μM) and 1 μl cDNA sample (about 200 ng), and 10.5 μl ddH₂O. Each reaction was performed in triplicate wells. Polymerase chain reaction (PCR) program was conducted on a Real-Time PCR System (ABI7500, Applied Biosystems) under the following conditions: 95°C for 1 min, followed by 35 cycles of 95°C for 20 s, then 56°C for 10 s and 72°C for 15 s. All abundances of the transcripts were normalized to U6 or GAPDH. The relative expression of gene was calculated with the $2^{-\Delta\Delta\text{Ct}}$ method. All primer sequences were provided in Supplemental Table 1.

Cell Transfection

Human GAS5 gene was amplified by PCR from hFOB1.19 cells and the cDNA sequences were subcloned into pcDNA3.1 vector (Sangon, Shanghai, China) to construct pcDNA-GAS5 plasmid, with the empty pcDNA3.1 vector serving as the negative control (Vector). Plasmids were transfected into HOS and U2OS cells using Lipofectamine 3000 Transfection Reagent, according to the manufacturer's instructions (Invitrogen, Carlsbad, CA, USA). MiR-23a-3p mimic, inhibitor, and its corresponding negative control mimic or inhibitor (NC-mimic and NC-inhibitor) were bought from Santa Cruz Biotechnology (Santa Cruz, CA, USA). In addition, siRNA negative control (Scramble), si-GAS5, and si-PTEN (all obtained from Sangon) were transfected into cells as described above.

Analysis of Cell Proliferation

Cell proliferation was detected by using CCK-8 assay. Briefly, cells were seeded into 96-well plates and cultured for 24 h. After transfection for 0, 24, 48, and 72 h, 10 μ l CCK-8 solution was added into each well and co-incubated with cells for another 2 h at 37°C. The absorption values were detected at wavelength of 450 nm with a microplate analyzer (Molecular Devices, Sunnyvale, CA, USA).

Invasion Assays

Cell invasion was determined using Matrigel™ Invasion Chambers. Briefly, 1×10^5 cells in 200 μ l serum-free DMEM were seeded into the upper compartment of 24-well plates, while 600 μ l medium, containing 20% FBS, was added to the lower chamber. After incubation for 48 h, cells on the upper membrane surface were removed using a cotton swab and invaded cells were fixed with 70% ethanol for 10 min and stained with 0.1% crystal violet for 15 min. These invasive cells were counted from five randomly selected fields using a light microscope (magnification, $\times 200$, Olympus, Tokyo).

Cell Apoptosis

Flow cytometry was used to evaluate cell apoptosis. After transfection, cells were collected and washed with phosphate-buffered saline for three times. Cells were stained with 5 μ l of Annexin V-FITC and 5 μ l of propidium iodide at room temperature in the dark for 20 min, and cell apoptosis was examined by using flow cytometry (BD Biosciences, Lake Franklin, NJ, USA).

RNA Immunoprecipitation and RNA Pull-down

RNA immunoprecipitation (RIP) assay was performed to explore the interaction between GAS5 and miR-23a-3p with EZ-Magna RIP RNA-binding protein immunoprecipitation kit (Millipore, Boston, MA, USA). After cells were lysed with RIP lysis buffer, 100 μ l of the lysate was incubated with RIP immunoprecipitation buffer containing magnetic beads, which were conjugated with human anti-Argonaute2 (Ago2) antibodies (Millipore, Billerica, MA, USA) or control normal mouse immunoglobulin G (IgG; Millipore, Billerica, MA, USA). Among the antibodies, IgG was considered as a negative control. Proteinase K buffer was then added to the samples to digest protein. Finally, the target RNA was extracted and purified for further study by using qPCR.

RNA pull-down assay was performed to examine the interaction between GAS5 and miR-23a-3p. Briefly, cells were transfected with biotinylated miRNA and collected. Then cell lysates were incubated with M-280 streptavidin magnetic beads (Invitrogen, San Diego, CA, USA). The bound RNAs were purified using TRIzol reagent (Invitrogen) for further qPCR analysis (the details about the amplified fragment and its primers are shown in Supplemental Fig. 1B).

Luciferase Reporter Gene Assay

The luciferase reporter gene assay was conducted on the basis of manufacturer's instructions. Using PCR, we amplified the putative miR-23a-3p target binding sites in GAS5 and the GAS5 mutant binding sequence. We then subcloned into a pmirGLO Reporter plasmid (Promega, Madison, WI, USA) to construct the wild-type GAS5 3'-untranslated region (UTR) (GAS5-WT), mutant GAS5 3'-UTR (GAS5-Mut), wild-type PTEN 3'-UTR (PTEN-WT), and mutant PTEN 3'-UTR (PTEN-Mut). Luciferase reporter plasmids and miR-23a-3p mimic or NC-mimic were cotransfected into HEK-293 T cells using Lipofectamine 3000. After transfection for 48 h, relative luciferase activity was measured by using a Dual-Luciferase Reporter Assay System (Promega).

Western Blotting

After transfection, cells were harvested and lysed in radio-immunoprecipitation assay lysis buffer (Beyotime, Shanghai, China) for 30 min at 4°C. Protein concentration was quantified by using an Enhanced BCA Protein Assay Kit (Beyotime). Protein samples were separated on 10% sodium dodecyl sulfate polyacrylamide gel electrophoresis and transferred to polyvinylidene difluoride membranes (Millipore, Bedford, MA, USA). After blocking with 5% skim milk for 1 h at room temperature, the blots were probed with primary antibodies overnight at 4°C [PTEN, 1:2,000 dilution; PI3 K, 1:1,000 dilution; phosphorylated PI3 K (p-PI3 K), 1:1,000 dilution; AKT, 1:1,000 dilution; phosphorylated AKT (p-AKT), 1:2,000 dilution] (Abcam, Cambridge, UK). Then the membranes were washed and incubated with secondary antibodies (1:2,000 dilution; Abcam, Cambridge, MA, USA) for 1 h at room temperature. Then, the chemiluminescent reagent was added to the membrane in an even manner and developed the image with a developing solution. All western blots were subjected to relative optical density analysis during the experiment. Finally, the signals were visualized using a chemiluminescence imaging system (Bioshine ChemiQ 4800 mini, Hangzhou, China; Haoxiang, Shanghai, China).

Tumor Xenograft Assay

All animals were approved by the Ethics Committee for the Use and Care of Animals of Shaanxi Provincial People's Hospital. Female BALB/c nude mice (age: 4 weeks old; weight: 16–20 g) were purchased from Institute of Laboratory Animals in Chinese Academy of Medical Sciences (Shanghai, China). The mice were randomly divided into two groups, and U2OS cells (2×10^6) containing pcDNA-GAS5 plasmid or pcDNA3.1 empty vector were subcutaneously injected into the right armpit of each mouse. Twenty-eight days later, the mice were sacrificed, and the cancer tissues were harvested. The tumor volume was calculated every week with the formula (mm^3): tumor volume = length \times width² \times 0.5. The body weight of the mice was

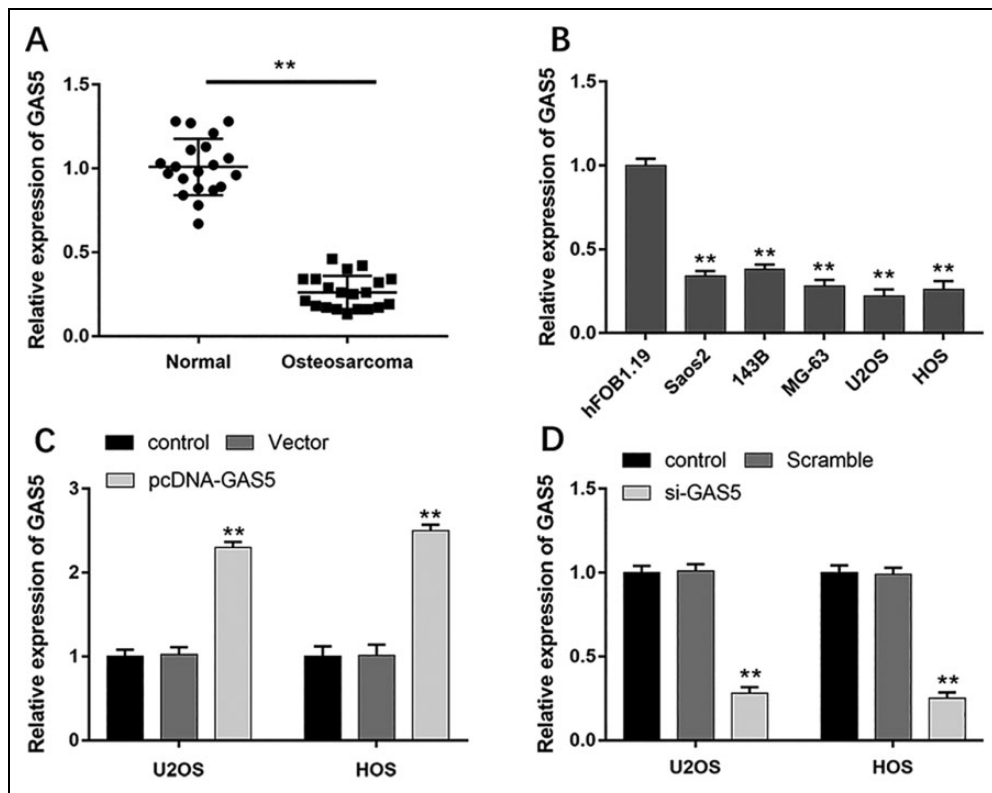


Figure 1. LncRNA GAS5 is downregulated in human osteosarcoma tissues and cell lines. (A) The expression of lncRNA GAS5 in human osteosarcoma tissues and matched adjacent tissues was detected by using qPCR ($n = 20$). (B) The levels of GAS5 in human normal osteoblast cells (hFOB1.19) and human OS cell lines (Saos2, 143B, MG-63, U2OS, and HOS) were measured by using qPCR. (C) The level of GAS5 was detected after transfection with 1 $\mu\text{g/ml}$ pcDNA-GAS5 for 48 h. (D) The expression of GAS5 was detected after transfection with 50 nM GAS5 siRNA (si-GAS5) for 48 h. ** $P < 0.01$ compared with adjacent tissues or hFOB1.19 cells. qPCR: quantitative polymerase chain reaction.

measured by using electronic scale every 7 days. The levels of GAS5 and miR-23a-3p in tumors were detected using qPCR, and the protein level of PTEN was analyzed using western blot.

Statistical Analysis

Data are reported as the mean \pm standard error of the mean and processed with SPSS version 22.0 software (IBM Corp., Armonk, NY, USA). *T*-test was used to compare the differences between the two groups. One-way analysis of variance was used for the difference analysis of three groups and more than three groups. $P < 0.05$ was considered to be statistically significant.

Results

LncRNA GAS5 is Downregulated in Osteosarcoma Tissues and Cell Lines

To define the potential function of GAS5 (transcript variant 2 in Supplemental Fig. 1A) in osteosarcoma progression, we first detected the levels of GAS5 in osteosarcoma tissues and matched adjacent tissues from 20 osteosarcoma patients by using reverse transcription-quantitative PCR (RT-qPCR).

And we found that the expression level of GAS5 in the osteosarcoma tissue was significantly lower than the adjacent tissue (Fig. 1A). Additionally, we also analyzed the expression of GAS5 in five osteosarcoma cell lines and a normal osteoblast cell line. The levels of GAS5 were dramatically downregulated in osteosarcoma cell lines Saos2, 143B, MG-63, U2OS, and HOS compared with hFOB1.19 (Fig. 1B). When cells were transfected with pcDNA-GAS5, the level of GAS5 observably increased relative to control group (Fig. 1C), while dramatically decreased after transfection with si-GAS5 (Fig. 1D). These results indicated that the level of GAS5 was downregulated in osteosarcoma.

Upregulation/Downregulation of GAS5 Inhibits/Promotes Osteosarcoma Proliferation and Invasion Through PI3K/AKT Signal Pathway

Since U2OS and HOS cells exhibited the lowest expression of GAS5, U2OS and HOS cells were selected for further analysis. CCK-8, Transwell, and flow cytometry assays showed that overexpression of GAS5 could suppress cell proliferation viability (Fig. 2A, B), reduce the number of

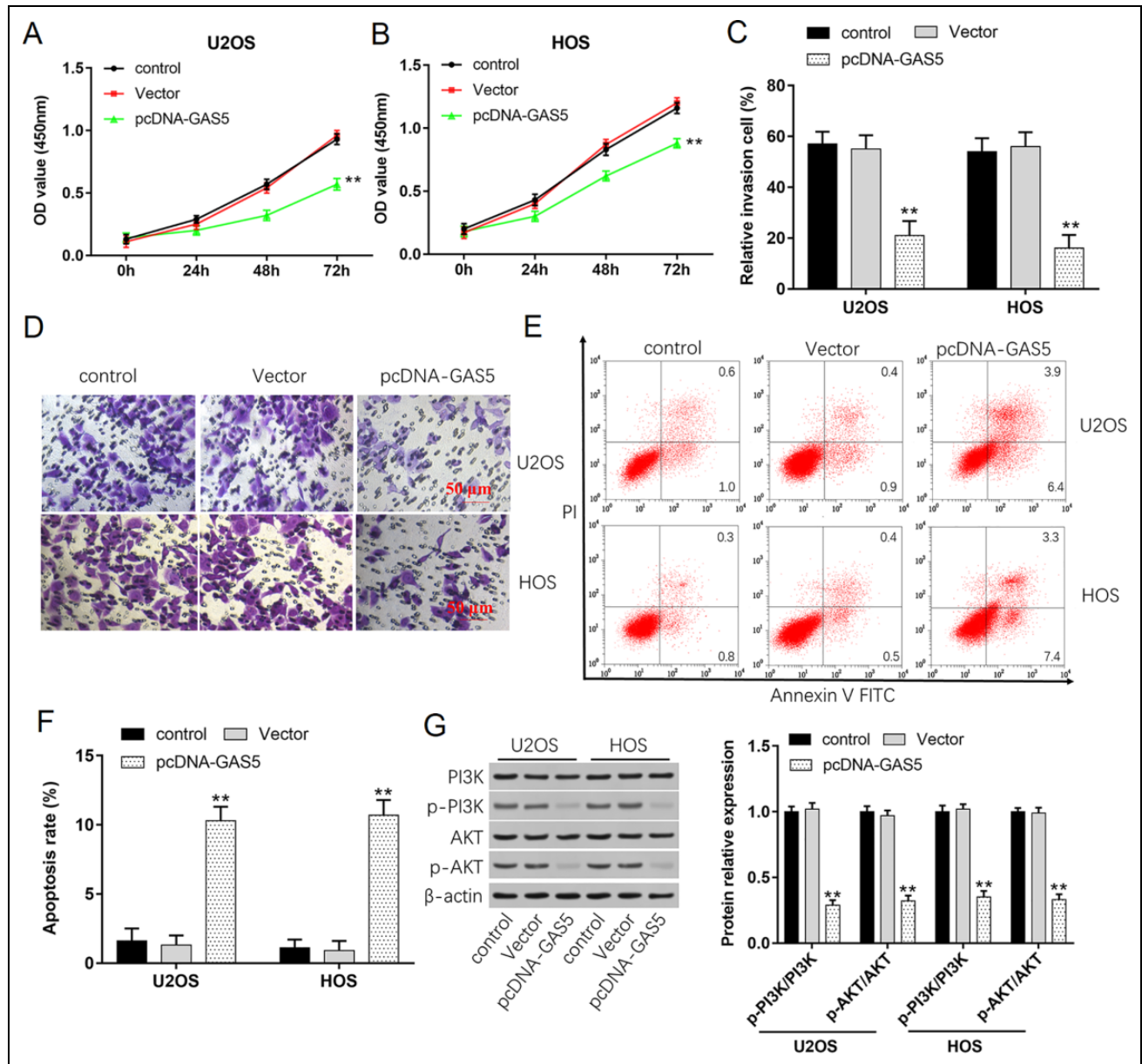


Figure 2. Overexpression of GAS5 inhibits cell growth, invasion, and PI3K/AKT signal pathway. (A, B) Proliferation of U2OS and HOS cells was detected by using CCK-8 assay after transfection with 1 μ g/ml pcDNA-GAS5 for 0, 24, 48, and 72 h. (C, D) The invasion ability of U2OS and HOS cells was evaluated by using Transwell invasion assay after transfection with pcDNA-GAS5 for 48 h. (E, F) Apoptosis rates of U2OS and HOS cells after transfection with pcDNA-GAS5 were detected by using flow cytometry. (G) Western blot analysis was used to detect the protein expression levels of PI3 K, p-PI3 K, AKT, and p-AKT after transfection with pcDNA-GAS5. * $P < 0.05$ and ** $P < 0.01$ compared with control.

cell invasion (Fig. 2C, D), and increase cell apoptosis (Fig. 2E, F), while downregulation of GAS5 could promote cell proliferation (Fig. 3A, B), increase cell invasion (Fig. 3C, D), and inhibit cell apoptosis (Fig. 3E, F). Western blot assay showed that the phosphorylation levels of PI3 K and AKT decreased after transfection with pcDNA-GAS5 (Fig. 2G) but increased after transfection with si-GAS5 (Fig. 3G). All results suggested that GAS5 was involved in the proliferation and invasion of osteosarcoma through PI3K/AKT signal pathway.

GAS5 is a Direct Target Gene of miR-23a-3p and Regulates the Expression of miR-23a-3p

LncRNA could inhibit the expression and activity of miRNA²³, so we used StarBase to predict the potential miRNA binding sites in GAS5. As shown in Fig. 4A, there is a complementary binding site between GAS5 and miR-23a-3p. To validate this prediction, luciferase reporter assay was performed. The luciferase activity of WT-GAS5 was significantly reduced by miR-23a-3p mimic in comparison

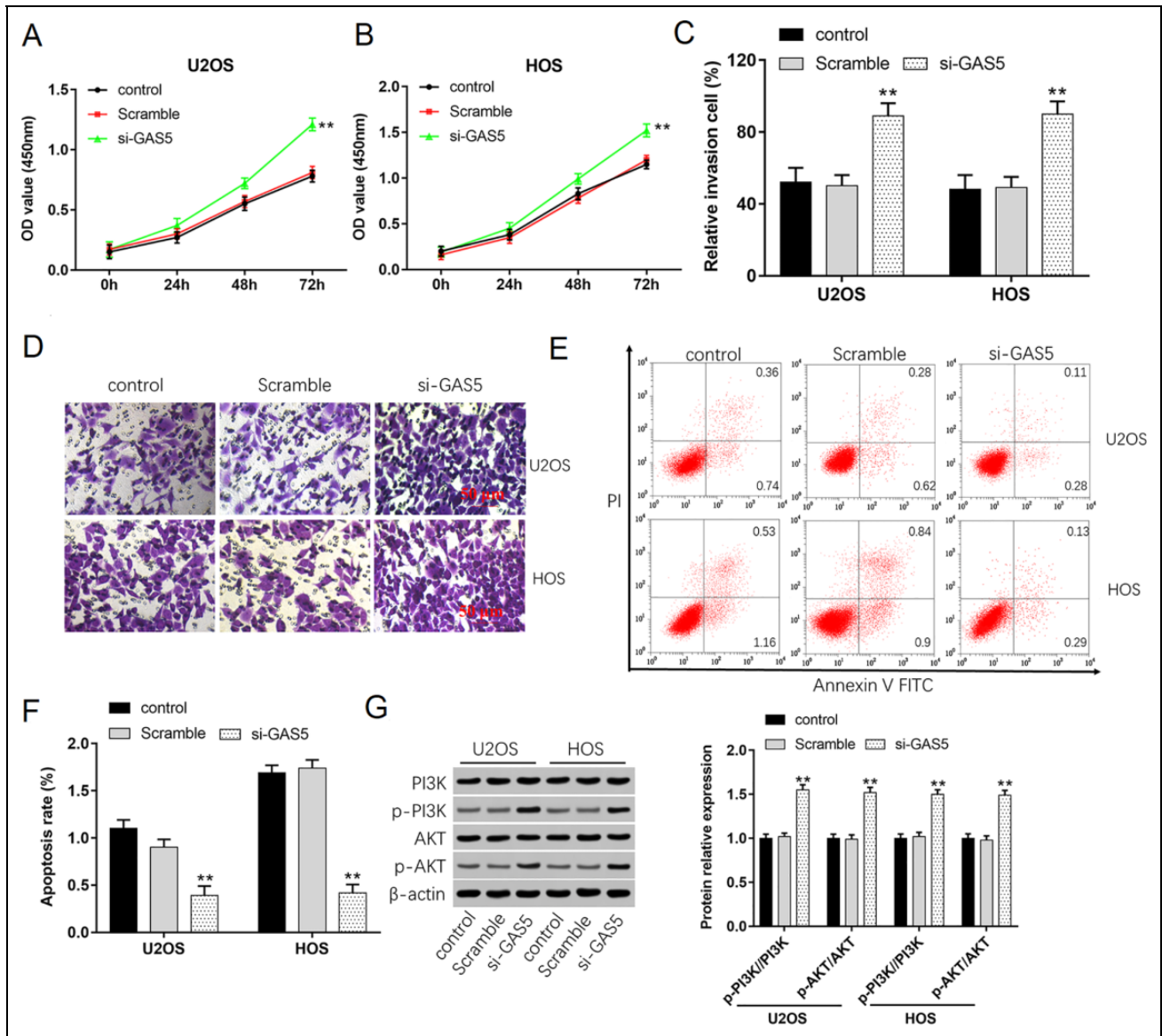


Figure 3. Downregulation of GAS5 promotes cell growth, invasion, and activates PI3K/AKT signal pathway. (A, B) Cell proliferation of U2OS and HOS cells was detected by using CCK-8 assay after transfection with si-GAS5 for 0, 24, 48, and 72 h. (C, D) The invasion ability of U2OS and HOS cells after transfection with si-GAS5 were detected by using Transwell invasion assay after transfection with si-GAS5 for 48 h. (E, F) Apoptosis rates of U2OS and HOS cells after transfection with si-GAS5 were detected by using flow cytometry. (G) Western blot analysis was used to detect the protein expression levels of PI3 K, p-PI3 K, AKT, and p-AKT after transfection with si-GAS5. $**P < 0.01$ compared with control.

with NC-mimic; however, there was no significant change in the Mut-GAS5 group (Fig. 4B). It has been proved that miRNAs exert their functions of gene silencing by recruiting nuclear localized Ago2. To conform whether GAS5 and miR-23a-3p are in the Ago2 immunoprecipitants, RIP assay was performed. IgG was used as the negative control. The results suggested that both GAS5 and miR-23a-3p were enriched in Ago2 pellet in comparison with IgG control group (Fig. 4C). Furthermore, a biotin-avidin pull-down assay was measured to analyze whether miR-23a-3p could pull down GAS5. The result revealed that GAS5 was pulled down by miR-23a-3p,

while failed to the mutated miR-23a-3p, suggesting that GAS5 could regulate miR-23a-3p in a sequence-specific manner (Fig. 4D). We also found that miR-23a-3p expression was higher in osteosarcoma tissues than that in adjacent tissues (Fig. 4E). The level of miR-23a-3p significantly upregulated in osteosarcoma cell lines (Fig. 4F). Moreover, the levels of miR-23a-3p were downregulated when U2OS and HOS cells were transfected with pcDNA-GAS5, while upregulated after transfection with si-GAS5 (Fig. 4G, H). These data indicated that GAS5 directly bound to miR-23a-3p and regulated the expression of miR-23a-3p.

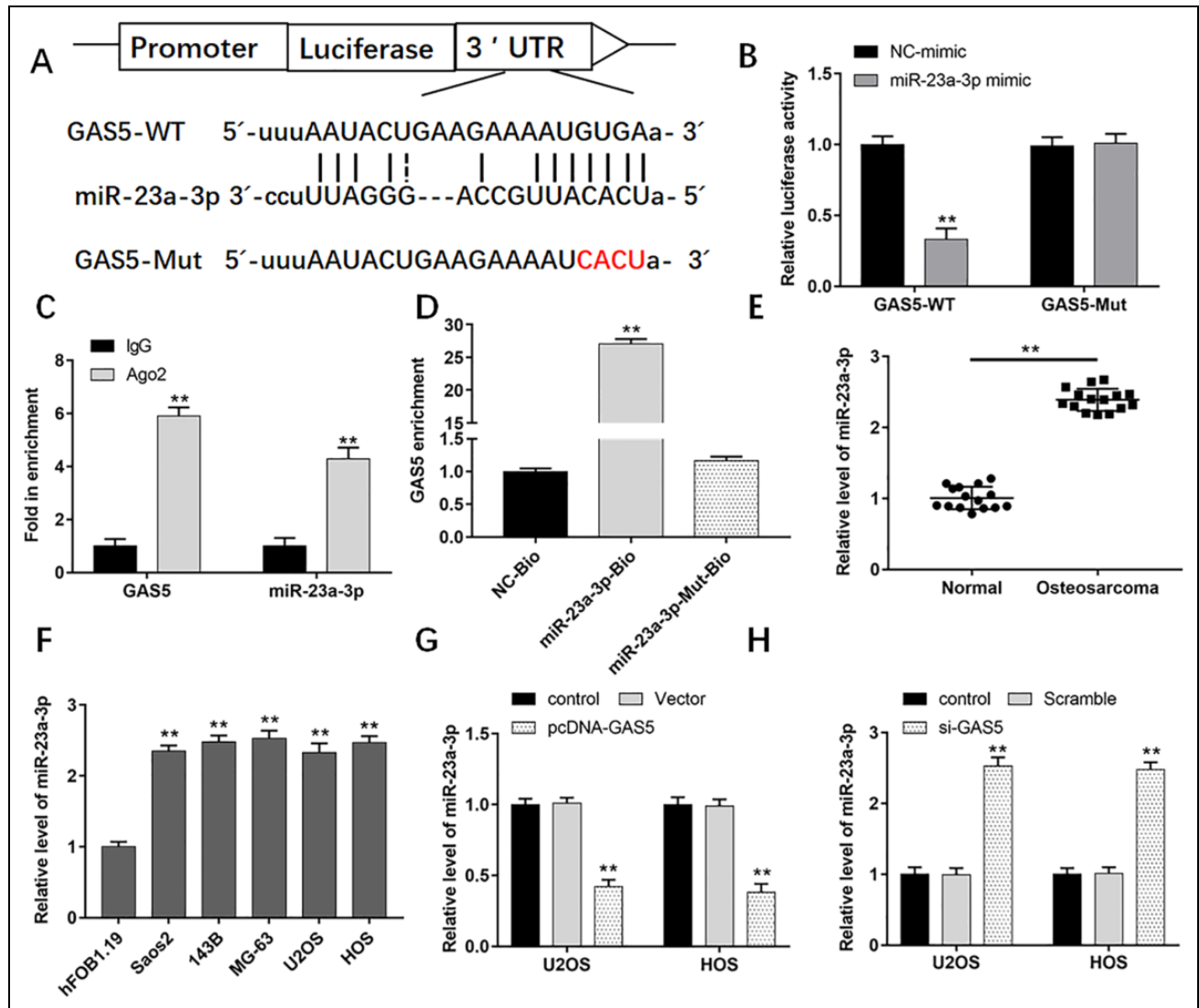


Figure 4. GAS5 is a direct target gene of miR-23a-3p and regulates expression of miR-23a-3p. (A) The binding sites of miR-23a-3p on GAS5 sequence. (B) Luciferase activities of GAS5-Wt and GAS5-Mut with or without transfection of miR-23a-3p. (C) RIP assay was conducted to examine the binding of miR-23a-3p in the Ago-precipitated RNA samples in different groups. (D) Fold enrichment of miR-23a-3p in the Ago-precipitated RNA samples in different groups. (E) The expression of miR-23a-3p in human osteosarcoma tissues and normal adjacent tissues was detected by using qPCR ($n = 20$). (F) The levels of miR-23a-3p in human osteoblast cells (hFOB1.19) and human OS cell lines (Saos2, 143B, MG-63, U2OS, and HOS) were measured by using qPCR. (G) The levels of miR-23a-3p in U2OS and HOS cells after transfection with pcDNA-GAS5 were detected by using qPCR. (H) The expression of miR-23a-3p in U2OS and HOS cells after transfection with si-GAS5 was detected by using qPCR. $**p < 0.01$ compared with adjacent tissues, hFOB1.19 cells, or control. qPCR: quantitative polymerase chain reaction; RIP: RNA immunoprecipitation.

Downregulation of miR-23a-3p Inhibits Cell Growth and Invasion Through Activating PI3K/AKT Signal Pathway

We conducted further studies on how miR-23a-3p regulated the proliferation and invasion of osteosarcoma cells. As shown in Fig. 5A, when U2OS and HOS cells were transfected with miR-23a-3p inhibitor, the levels of miR-23a-3p remarkably reduced. And the proliferation ability of cells decreased obviously compared with NC-inhibitor group

(Fig. 5B, C). Transwell assay showed that the number of cell invasion decreased after transfection with miR-23a-3p inhibitor (Fig. 5D). Cell apoptosis was determined using flow cytometry. The results demonstrated that downregulation of miR-23a-3p could significantly promote cell apoptosis (Fig. 5E, F). Western blot experiments showed that downregulation of miR-23a-3p could reduce the phosphorylation of PI3K and AKT (Fig. 5G). These results indicated that miR-23a-3p promoted cell proliferation and invasion by activating PI3K/AKT signal pathway.

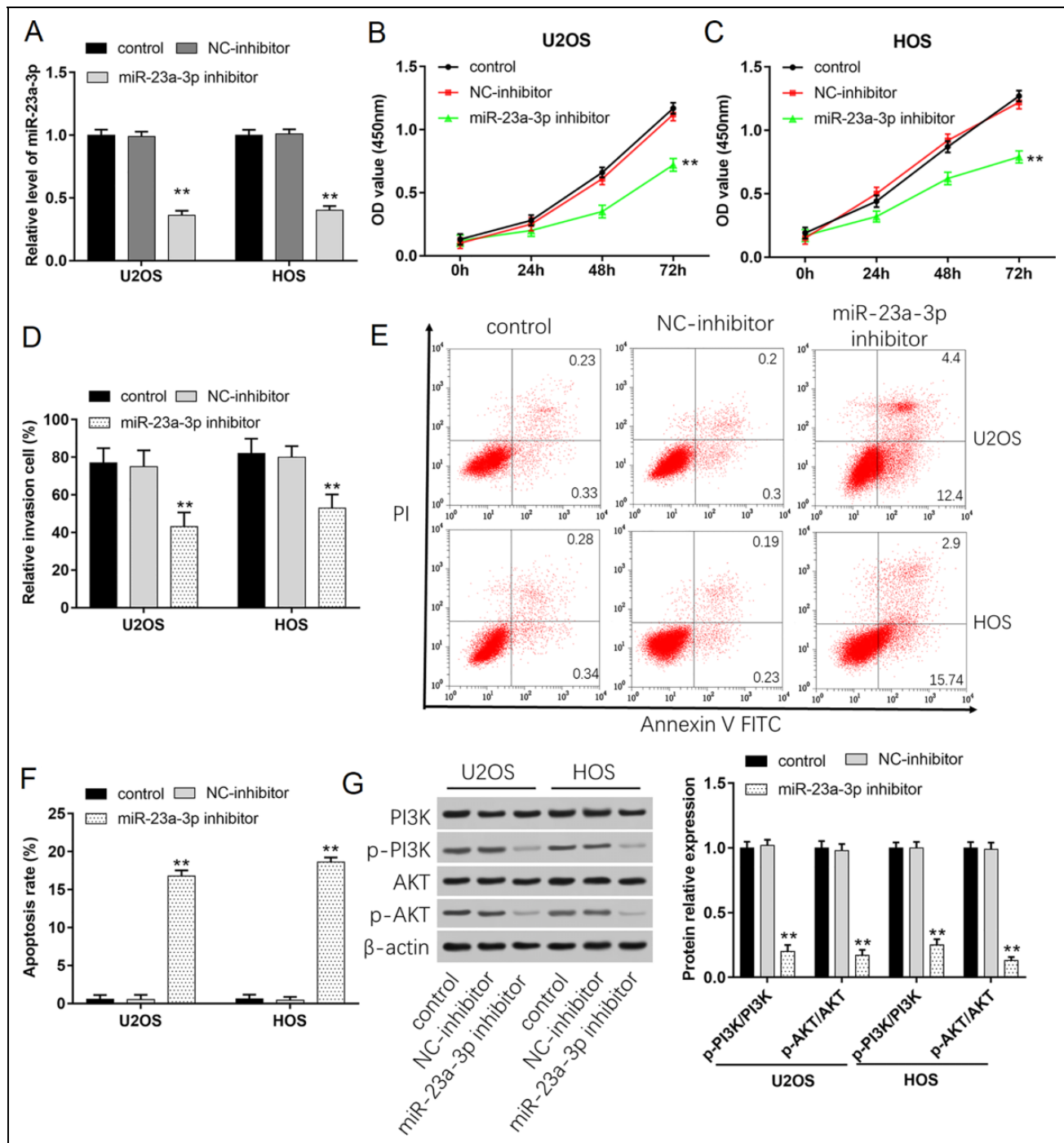


Figure 5. Downregulation of miR-23a-3p inhibits cell growth and invasion through activating the PI3K/AKT signaling pathway. U2OS and HOS cells were transfected with 40 nM NC-inhibitor or 40 nM miR-23a-3p inhibitor. (A) Transfection efficiencies were detected by using qPCR. (B, C) Cell proliferation of U2OS and HOS cells was detected by using CCK-8 assay. (D) The invasion ability of U2OS and HOS cells was evaluated by using Transwell invasion assay. (E, F) Apoptosis of U2OS and HOS cells was detected by using flow cytometry. (G) Western blot analysis was used to detect the protein expression levels of PI3K, p-PI3K, AKT, and p-AKT. ** $P < 0.01$ compared with Vector and NC-mimic. qPCR: quantitative polymerase chain reaction.

PTEN is a Target Gene of miR-23a-3p in Osteosarcoma Cells

By utilizing StarBase, we found that miR-23a-3p could potentially target PTEN (Fig. 6A). Luciferase assay

indicated that miR-23a-3p mimic significantly inhibited the luciferase activity in WT-PTEN group ($P < 0.01$), but not completely inhibited the luciferase activity in Mutant1 or Mutant2 of PTEN groups. When both binding sites were

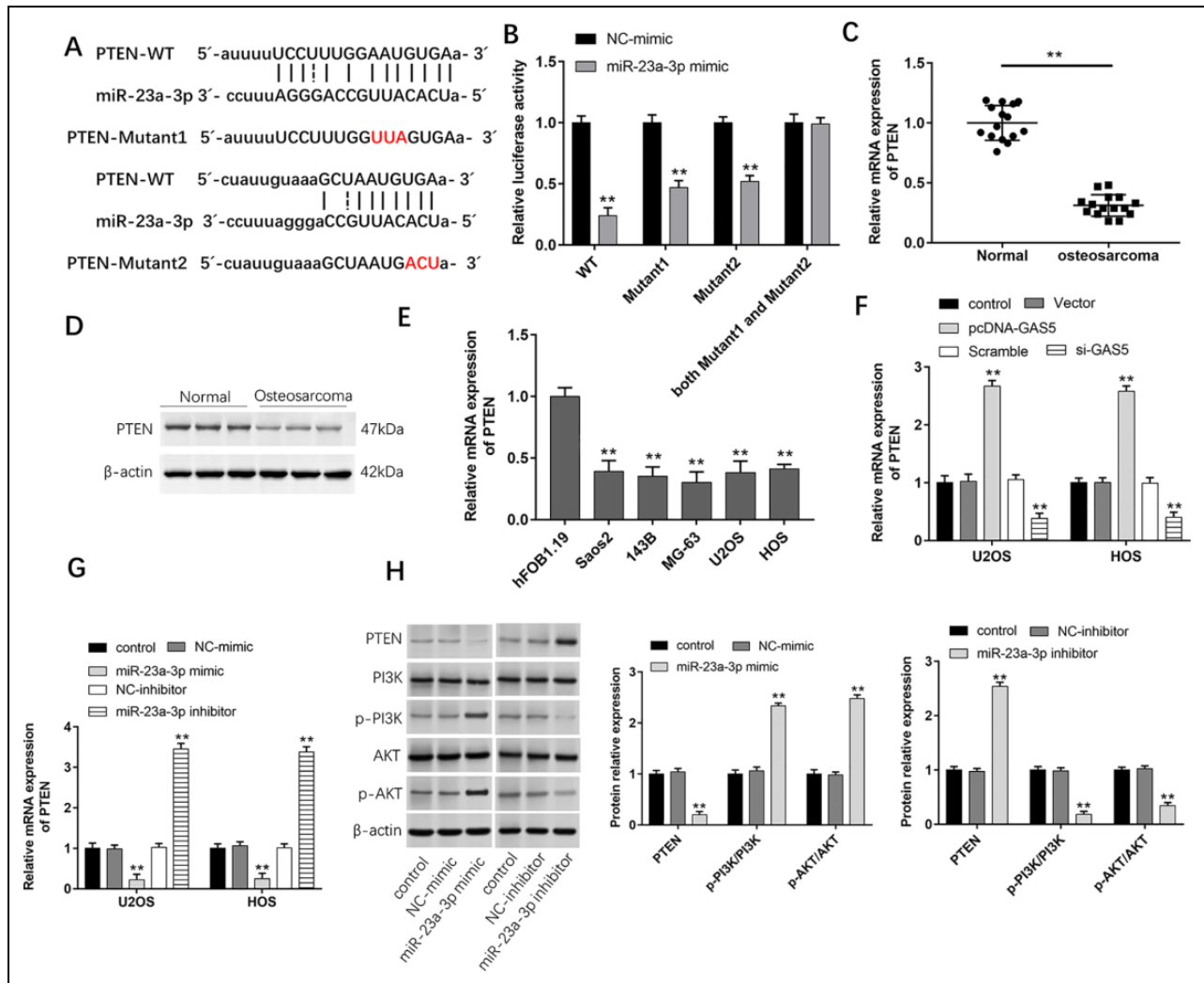


Figure 6. PTEN is a target gene of miR-23a-3p. (A) The predicted binding sites between miR-23a-3p and PTEN. (B) The relative luciferase activity in HEK-293 T cells cotransfected with the miR-23a-3p mimic and either of the luciferase reporter vectors containing PTEN-WT, PTEN-Mutant I, PTEN-Mutant2, and NC-mimic. (C, D) The expression of PTEN in human osteosarcoma tissues and normal adjacent tissues was detected by using qPCR ($n = 15$). (E) The mRNA level of PTEN in human osteoblast cells (hFOB1.19) and human OS cell lines (Saos2, 143B, MG-63, U2OS, and HOS). (F, G) The mRNA levels of PTEN in U2OS and HOS cells after transfected with pcDNA-GAS5, si-GAS5, miR-23a-3p mimic, or miR-23a-3p inhibitor were detected by using qPCR. (H) The protein levels of PTEN, PI3 K, p-PI3 K, AKT, and p-AKT in U2OS cells were detected with Western blotting. $**P < 0.01$ compared with NC-mimic, normal tissues, hFOB1.19 cells, or Vector and NC-mimic. PTEN: phosphatase and tensin homolog; qPCR: quantitative polymerase chain reaction.

mutated at the same time, luciferase activity was basically unaffected (Fig. 6B). We also analyzed the mRNA and protein levels of PTEN in osteosarcoma tissue samples and the corresponding adjacent tissues. The results found that the levels of PTEN in osteosarcoma tissues were significantly lower than these in adjacent tissues (Fig. 6C, D). The levels of PTEN were also downregulated in osteosarcoma cell lines compared with hFOB1.19 (Fig. 6E). Moreover, PTEN expression obviously increased in pcDNA-GAS5 and miR-23a-3p inhibitor groups, while decreased in si-GAS5 and miR-23a-3p mimic group (Fig. 6F, G). In addition, western blot revealed that upregulation of miR-23a-3p repressed the protein levels of PTEN, but promoted the expression of phosphorylated PI3 K and AKT (Fig. 6H). Silence of miR-

23a-3p showed the opposite results. These findings revealed that PTEN was a target gene of miR-23a-3p.

GAS5 Inhibits Osteosarcoma Cell Proliferation and Invasion via miR-23a-3p/PTEN/PI3K/AKT Pathway in U2OS and HOS Cells

To explore the relationship among GAS5, miR-23a-3p, and PTEN, U2OS and HOS cells were transfected with Vector, pcDNA-GAS5, pcDNA-GAS5 and NC-mimic, pcDNA-GAS5 and miR-23a-3p mimic, and pcDNA-GAS5 and Scramble, or pcDNA-GAS5 and si-PTEN. Cell proliferation results showed that overexpression of GAS5 could inhibit

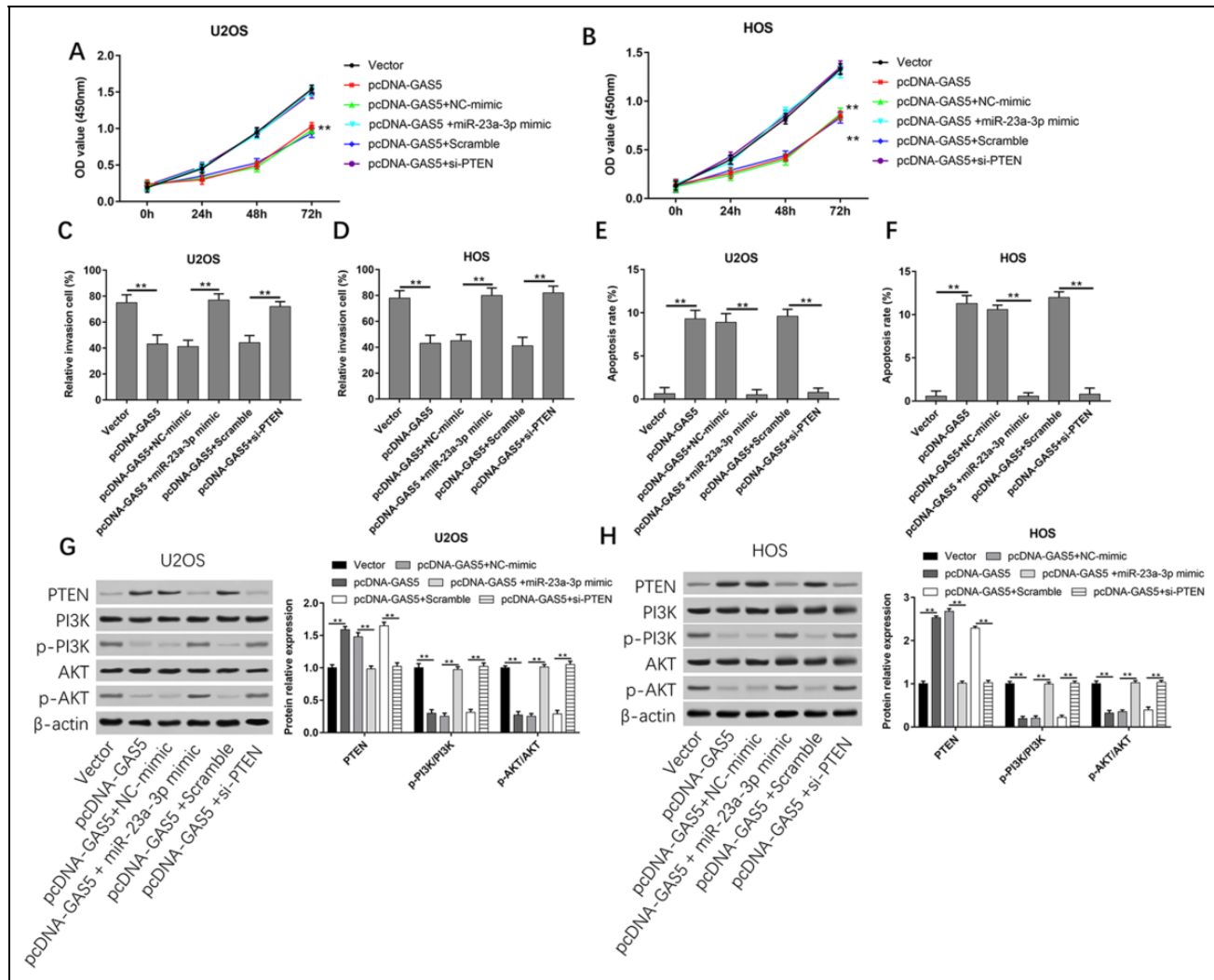


Figure 7. GAS5 inhibits osteosarcoma cell migration and invasion via miR-23a-3p/PTEN/PI3K/AKT pathway. U2OS and HOS cells were respectively transfected with Vector, pcDNA-GAS5, pcDNA-GAS5 and NC-mimic, pcDNA-GAS5 and miR-23a-3p mimic, and pcDNA-GAS5 and Scramble, or pcDNA-GAS5 and si-PTEN for 48 h. (A, B) Cell proliferation of U2OS and HOS cells was detected by using CCK-8 assay. (C, D) The invasion ability of U2OS and HOS cells was evaluated by using Transwell invasion assay. (E, F) Apoptosis of U2OS and HOS cells was detected by using flow cytometry. (G, H) Western blot analysis was used to detect the protein expression levels of PTEN, PI3K, p-PI3K, AKT, and p-AKT. $**P < 0.01$ compared with Vector and Scramble. PTEN: phosphatase and tensin homolog.

cell growth, while overexpression of miR-23a-3p or silence of PTEN could reverse the inhibitory effect by GAS5 (Fig. 7A, B). Data in Fig. 7C–F showed that cells cotransfected with pcDNA-GAS5 and NC-mimic significantly decreased cell invasion but increased cell apoptotic ($P < 0.01$). However, cotransfection with pcDNA-GAS5 and miR-23a-3p mimic or pcDNA-GAS5 and si-PTEN could counteract the decrease of cell invasion and the increase of cell apoptosis. As shown in Fig. 7G, H, overexpression of GAS5 significantly increased the protein levels of PTEN, while reduced the phosphorylated levels of PI3K and AKT ($P < 0.01$). However, in relation to the Vector group, the protein levels of PTEN and phosphorylated PI3K and AKT did not change remarkably. These data suggested that overexpression of GAS5 inhibited osteosarcoma cell migration and invasion

by downregulating the expression of miR-23a-3p and upregulating PTEN level to inhibit the activation of PI3K/AKT pathway in osteosarcoma cells.

Overexpression of GAS5 Inhibits the Tumorigenesis of Osteosarcoma In Vivo

In the in vivo experiments, overexpression of GAS5 could significantly suppress tumor growth. Compared with Vector group, pcDNA-GAS5 group had smaller tumor size and lighter weight (Fig. 8A–C). RT-qPCR data demonstrated that the level of GAS5 was higher than that in Vector group, while miR-23a-3p expression was reduced (Fig. 8D, E). Western blot results showed that the protein expression of PTEN was increased in pcDNA-GAS5 group (Fig. 8F). Our

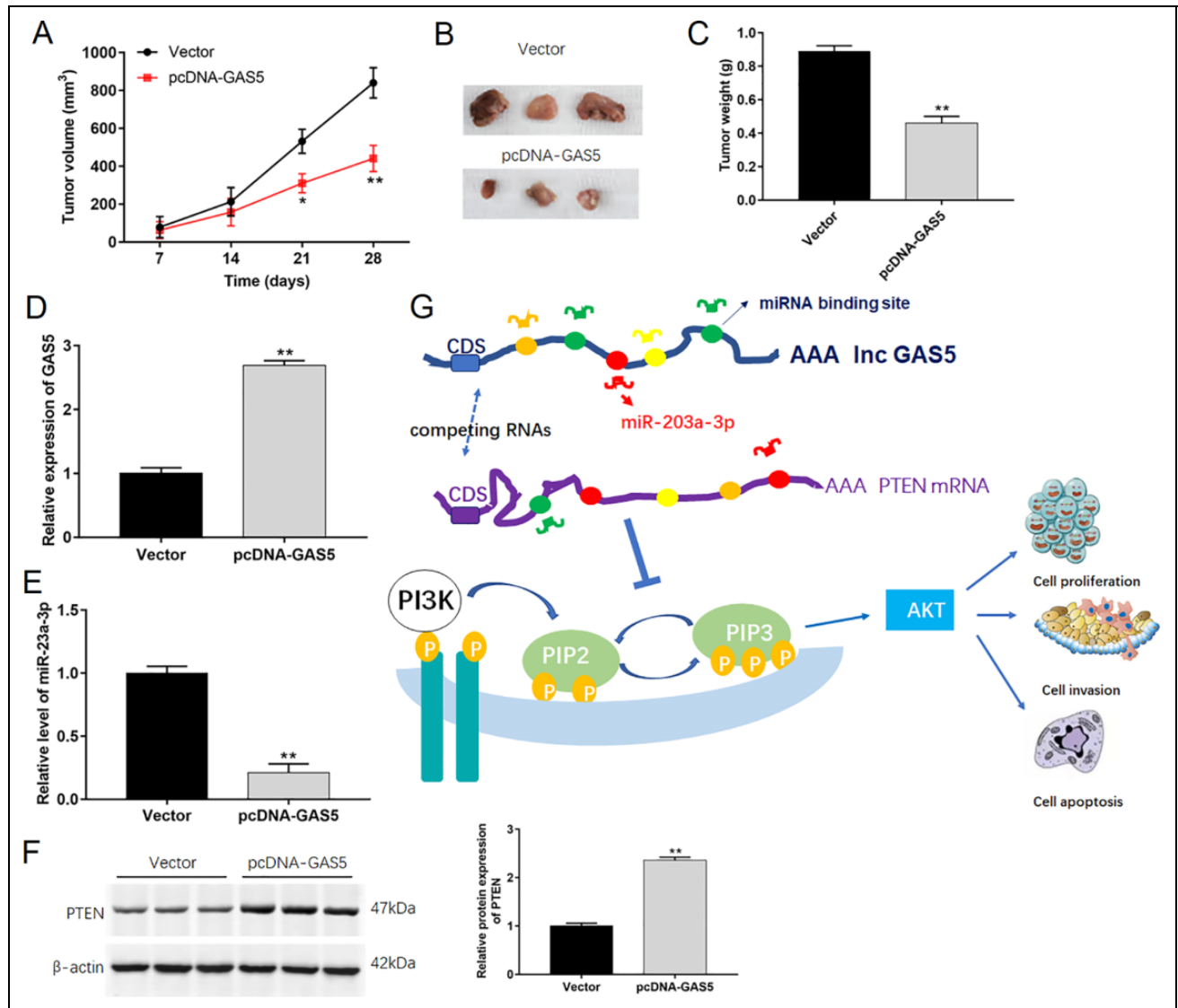


Figure 8. Overexpression of GAS5 inhibits the tumorigenesis of osteosarcoma in vivo. Subcutaneous tumor transplantation model was established by injection with U2OS cells that were transfected with empty vector or pcDNA-GAS5 expression vector. (A) Tumor volumes were calculated every 7 days. (B) Representative pictures of the tumors from each group at day 28. (C) The weight of tumors was determined at day 28. The levels of (D) GAS5 and (E) miR-23a-3p were detected by using qPCR. (F) The protein level of PTEN was analyzed by using Western blot analysis. (G) A schematic diagram for the role of GAS5/miR-23a-3p/PTEN/PI3K/AKT pathway in regulating osteosarcoma progression. ** $P < 0.01$ compared with Vector. PTEN: phosphatase and tensin homolog; qPCR: quantitative polymerase chain reaction.

findings indicated that the lncRNA GAS5 competitively binds with miR-23a-3p that could post-transcriptionally suppressed the expression of the tumor suppressor gene PTEN, thus inhibiting the activation of the pathway PI3K/AKT to suppress proliferation and invasion and promote apoptosis in osteosarcoma cells (Fig. 8G).

Discussion

Disorders of lncRNAs have been shown to be involved in the development and progression of many human

diseases. GAS5 also plays an important regulatory role in pathophysiological process. For instance, GAS5 was upregulated in atherosclerosis, suggesting that GAS5 implicated in the development of atherosclerosis²⁴. Moreover, the expression levels of GAS5 were remarkably increased in epilepsy and ischemic heart disease^{25,26}. Additionally, in this study, we found that GAS5 expression significantly downregulated in osteosarcoma, which was also consistent with some literature reports. GAS5 was downregulated in gastric tissues and cell lines²⁷, and GAS5 also was downregulated in diabetic nephropathy²⁸.

The inconsistency may be attributed to the different pathogenesis of different diseases.

Overexpression of GAS5 could inhibit the proliferation, invasion, and promote apoptosis of osteosarcoma cells, which fully indicated that GAS5 acted as a tumor suppressor in osteosarcoma cells. However, the mechanism how GAS5 inhibited osteosarcoma growth and metabolism was unclear. GAS5 has been reported to interact with miRNAs to participate in the process of tumorigenesis. Reports had indicated that GAS5 inhibited laryngeal squamous cell proliferation by reversing ectopic expression of miR-21²⁹. Other reports revealed that GAS5 prevented human B lymphocytic leukemia tumorigenesis and metastasis by sponging miR-222³⁰. However, we found that GAS5 could interact with miR-23a-3p through luciferase reporter gene and RNA immunoprecipitation. It has been demonstrated that miR-23a-3p could act as an oncogene²¹. Overexpression of GAS5 could suppress the expression of miR-23a-3p. Therefore, we hypothesized that GAS5 may inhibit tumor proliferation and invasion by inhibiting the expression of miR-23a-3p.

It has been suggested that miRNAs could post-transcriptionally control genes expression by targeting the 3'-UTRs of mRNAs. Studies have reported that the expression and function of miR-23a-3p are different in various pathological tissues. MiR-23a-3p was downregulated in oral squamous cell carcinomas and inhibited the expression of fibroblast growth factor 2 to suppress cell proliferation³¹. However, high expression of miR-23a-3p promoted tumorigenesis by inhibiting Proline-Rich Nuclear Receptor Coactivator 2 in renal cell carcinoma²¹. PTEN is well known to function as a tumor suppressor gene in the initiation and development of cancer. In this study, we conducted luciferase reporter gene assay to validate that PTEN was a target gene of miR-23a-3p. And miR-23a-3p could target and downregulate the level of PTEN in osteosarcoma cells.

Signaling pathway plays an important role in the occurrence and development of human tumors. Previous studies had displayed that GAS5 might inhibit the proliferation of mesangial cells and accumulation of extracellular matrix via nuclear transcription factor- κ B pathway³². Song et al. reported that GAS5 inhibited angiogenesis and metastasis of colorectal cancer through the Wnt/ β -catenin signaling pathway³³. PTEN mainly acts on the downstream target molecule PIP3 of PI3 K through its lipid phosphatase activity, thereby blocking the PI3K/AKT signaling pathway to achieve its anticancer effect. Therefore, in this article, we wondered whether GAS5 could inhibit cell proliferation and invasion in osteosarcoma cells through the PTEN/PI3K/AKT signaling pathway. The findings revealed that overexpression of GAS5 suppressed the levels of miR-23a-3p, p-PI3 K, and p-AKT, while increased the level of PTEN, suggesting that GAS5 was involved in the development of osteosarcoma through PI3K/AKT signaling pathway.

In vivo xenograft experiments showed that overexpression of GAS5 could suppress the growth of osteosarcoma and the expression of miR-23a-3p, while upregulate the level

of PTEN. Based on the findings acquired from this study, overexpression of GAS5 could inhibit osteosarcoma cell proliferation and invasion by miR-23a-3p/PTEN/PI3K/AKT pathway. Targeting the GAS5/miR-23a-3p/PTEN interaction may represent a novel therapeutic perspective and contribute to a better knowledge of the molecular mechanism of osteosarcoma.

Availability of Data Materials

The datasets used during the present study are available from the corresponding author upon reasonable request.

Ethical Approval

The protocols were approved by the Ethics Committee of Shaanxi Provincial People's Hospital.

Statement of Human and Animal Rights

All procedures involving the care and use of laboratory animals were approved by the Animal Policy and Welfare Committee of Shaanxi Provincial People's Hospital, and all efforts were made to minimize use of animals as well as to minimize their pain or discomfort during the course of the study.

Statement of Informed Consent

Written informed consent was obtained from the patients for their anonymized information to be published in this article.

Authors' Contributions

JL performed the experiments and prepared the manuscript, MC designed the study, LM and XD prepared the figures, and GD performed the statistical analysis.


Declaration of Conflicting Interests

The author(s) declared no potential conflicts of interest with respect to the research, authorship, and/or publication of this article.

Funding

The author(s) received no financial support for the research, authorship, and/or publication of this article.

ORCID iD

Ming Chen  <https://orcid.org/0000-0002-2487-3514>

Supplemental Material

Supplemental material for this article is available online.

References

1. Wei CJ, Li YL, Zhu ZL, Jia DM, Fan ML, Li T, Wang XJ, Li ZG, Ma HS. Inhibition of activator protein 1 attenuates neuroinflammation and brain injury after experimental intracerebral hemorrhage. *CNS Neurosci Ther.* 2019;25(10):1182–1188.
2. Fei D, Zhang X, Liu J, Tan L, Xing J, Zhao D, Zhang Y. Long noncoding RNA FER1L4 suppresses tumorigenesis by regulating the expression of PTEN targeting miR-18a-5p in osteosarcoma. *Cell Physiol Biochem.* 2018;51(3):1364–1375.
3. Li WT, Zhang Q. MicroRNA-708-5p regulates mycobacterial vitality and the secretion of inflammatory factors in

- Mycobacterium tuberculosis-infected macrophages by targeting TLR4. *Eur Rev Med Pharmacol Sci.* 2019;23(18):8028–8038.
4. Gu Q, Luo Y, Chen C, Jiang D, Huang Q, Wang X. GREM1 overexpression inhibits proliferation, migration and angiogenesis of osteosarcoma. *Exp Cell Res.* 2019;384(1):111619.
 5. Wang Y, Kong D. LncRNA GAS5 represses osteosarcoma cells growth and metastasis via sponging MiR-203a. *Cell Physiol Biochem.* 2018;45(2):844–855.
 6. Wang W, Li J, Ding Z, Li Y, Wang J, Chen S, Miao J. Tan-shinone I inhibits the growth and metastasis of osteosarcoma via suppressing JAK/STAT3 signalling pathway. *J Cell Mol Med.* 2019;23(9):6454–6465.
 7. Zhang X, Du K, Lou Z, Ding K, Zhang F, Zhu J, Chang Z. The CtBP1-HDAC1/2-IRF1 transcriptional complex represses the expression of the long noncoding RNA GAS5 in human osteosarcoma cells. *Int J Biol Sci.* 2019;15(7):1460–1471.
 8. Xin Y, Lyu X, Wang C, Fu Y, Zhang S, Tian C, Li Q, Zhang D. Elevated circulating levels of CTRP1, a novel adipokine, in diabetic patients. *Endocr J.* 2014;61(9):841–847.
 9. Lu L, Zhang RY, Wang XQ, Liu ZH, Shen Y, Ding FH, Meng H, Wang LJ, Yan XX, Yang K, Wang HB, et al. C1q/TNF-related protein-1: an adipokine marking and promoting atherosclerosis. *Eur Heart J.* 2016;37(22):1762–1771.
 10. Wen Q, Liu Y, Lyu H, Xu X, Wu Q, Liu N, Yin Q, Li J, Sheng X. Long noncoding RNA GAS5, which acts as a tumor suppressor via microRNA 21, regulates cisplatin resistance expression in cervical cancer. *Int J Gynecol Cancer.* 2017;27(6):1096–1108.
 11. Gao ZQ, Wang JF, Chen DH, Ma XS, Wu Y, Tang Z, Dang XW. Long non-coding RNA GAS5 suppresses pancreatic cancer metastasis through modulating miR-32-5p/PTEN axis. *Cell Biosci.* 2017;7(1):66.
 12. Dong S, Zhang X, Liu D. Overexpression of long noncoding RNA GAS5 suppresses tumorigenesis and development of gastric cancer by sponging miR-106a-5p through the Akt/mTOR pathway. *Biol Open.* 2019;8(6):bio041343.
 13. Fan YZ, Huang H, Wang S, Tan GJ, Zhang QZ. Effect of lncRNA MALAT1 on rats with myocardial infarction through regulating ERK/MAPK signaling pathway. *Eur Rev Med Pharmacol Sci.* 2019;23(20):9041–9049.
 14. Vo DT, Karanam NK, Ding L, Saha D, Yordy JS, Giri U, Heymach JV, Story MD. miR-125a-5p functions as tumor suppressor microRNA and is a marker of locoregional recurrence and poor prognosis in head and neck cancer. *Neoplasia.* 2019;21(9):849–862.
 15. Zhang Y, Zhang D, Lv J, Wang S, Zhang Q. MiR-125a-5p suppresses bladder cancer progression through targeting FUT4. *Biomed Pharmacother.* 2018;108:1039–1047.
 16. Jia J, Zhang M, Li Q, Zhou Q, Jiang Y. Long noncoding ribonucleic acid NKILA induces the endoplasmic reticulum stress/autophagy pathway and inhibits the nuclear factor-k-gene binding pathway in rats after intracerebral hemorrhage. *J Cell Physiol.* 2018;233(11):8839–8849.
 17. Sun L, Liu M, Luan S, Shi Y, Wang Q. MicroRNA-744 promotes carcinogenesis in osteosarcoma through targeting LATS2. *Oncol Lett.* 2019;18(3):2523–2529.
 18. Dorn GW II, Matkovich SJ. Menage a Trois: intimate relationship among a microRNA, long noncoding RNA, and mRNA. *Circ Res.* 2014;114(9):1362–1365.
 19. Cui H, Zhao J. LncRNA TMPO-AS1 serves as a ceRNA to promote osteosarcoma tumorigenesis by regulating miR-199a-5p/WNT7B axis. *J Cell Biochem.* 2020;121(3):2284–2293.
 20. Li K, Zhao B, Wei D, Cui Y, Qian L, Wang W, Liu G. Long non-coding RNA ANRIL enhances mitochondrial function of hepatocellular carcinoma by regulating the MiR-199a-5p/ARL2 axis. *Environ Toxicol.* 2020;35(3):313–321.
 21. Quan J, Pan X, Li Y, Hu Y, Tao L, Li Z, Zhao L, Wang J, Li H, Lai Y, Zhou L, et al. MiR-23a-3p acts as an oncogene and potential prognostic biomarker by targeting PNCRC2 in RCC. *Biomed Pharmacother.* 2019;110:656–666.
 22. Chen G, Li Y, He Y, Zeng B, Yi C, Wang C, Zhang X, Zhao W, Yu D. Upregulation of circular RNA circATRNL1 to sensitize oral squamous cell carcinoma to irradiation. *Mol Ther Nucleic Acids.* 2020;19:961–973.
 23. Jalali S, Bhartiya D, Lalwani MK, Sivasubbu S, Scaria V. Systematic transcriptome wide analysis of lncRNA-miRNA interactions. *PLoS One.* 2013;8(2):e53823.
 24. Lewis TA, Taylor FR, Parks LW. Involvement of heme biosynthesis in control of sterol uptake by *Saccharomyces cerevisiae*. *J Bacteriol.* 1985;163(1):199–207.
 25. Li BG, Wu WJ, Zheng HC, Yang HF, Zuo YX, Cui XP. Long noncoding RNA GAS5 silencing inhibits the expression of KCNQ3 by sponging miR-135a-5p to prevent the progression of epilepsy. *Kaohsiung J Med Sci.* 2019;35(9):527–534.
 26. Wu N, Zhang X, Bao Y, Yu H, Jia D, Ma C. Down-regulation of GAS5 ameliorates myocardial ischaemia/reperfusion injury via the miR-335/ROCK1/AKT/GSK-3beta axis. *J Cell Mol Med.* 2019;23(12):8420–8431.
 27. Liu Y, Yin L, Chen C, Zhang X, Wang S. Long non-coding RNA GAS5 inhibits migration and invasion in gastric cancer via interacting with p53 protein. *Dig Liver Dis.* 2020;52(3):331–338.
 28. Ge X, Xu B, Xu W, Xia L, Xu Z, Shen L, Peng W, Huang S. Long noncoding RNA GAS5 inhibits cell proliferation and fibrosis in diabetic nephropathy by sponging miR-221 and modulating SIRT1 expression. *Aging (Albany NY)* 2019;11(20):8745–8759.
 29. Lyu K, Xu Y, Yue H, Li Y, Zhao J, Chen L, Wu J, Zhu X, Chai L, Li C, Wen W, et al. Long noncoding RNA GAS5 acts as a tumor suppressor in laryngeal squamous cell carcinoma Via miR-21. *Cancer Manag Res.* 2019;11(17):8487–8498.
 30. Jing Z, Gao L, Wang H, Chen J, Nie B, Hong Q. Long non-coding RNA GAS5 regulates human B lymphocytic leukaemia tumorigenesis and metastasis by sponging miR-222. *Cancer Biomark.* 2019;26(3):385–392.

31. Chen F, Qi S, Zhang X, Wu J, Yang X, Wang R. miR-23a-3p suppresses cell proliferation in oral squamous cell carcinomas by targeting FGF2 and correlates with a better prognosis: miR-23a-3p inhibits OSCC growth by targeting FGF2. *Pathol Res Pract.* 2019;215(4):660–667.
32. Zhang R, Han X, Huang T, Wang X. Danggui buxue tang inhibited mesangial cell proliferation and extracellular matrix accumulation through GAS5/NF-kappaB pathway. *Biosci Rep.* 2019;39(10):BSR20181740.
33. Song J, Shu H, Zhang L, Xiong J. Long noncoding RNA GAS5 inhibits angiogenesis and metastasis of colorectal cancer through the Wnt/beta-catenin signaling pathway. *J Cell Biochem.* 2019;120(5):6937–6951.